PHYSICAL REVIEW B **79**, 020408(R) (2009)

Field-controlled magnetic order in the quantum spin-ladder system $(Hpip)_2CuBr_4$

B. Thielemann,[1] Ch. Rüegg,[2] K. Kiefer,[3] H. M. Rønnow,[4] B. Normand,[5] P. Bouillot,[6] C. Kollath,[7] E. Orignac,[8] R. Citro,[9] T. Giamarchi,[6] A. M. Läuchli,[10] D. Biner,[11] K. W. Krämer,[11] F. Wolff-Fabris,[12] V. S. Zapf,[12] M. Jaime,[12] J. Stahn,[1] N. B. Christensen,[1,13] B. Grenier,[14] D. F. McMorrow,[2] and J. Mesot[1,4]

[1]*Laboratory for Neutron Scattering, ETH Zurich and Paul Scherrer Institute, CH-5232 Villigen, Switzerland*

[2]*London Centre for Nanotechnology and Department of Physics and Astronomy, University College London, London WC1E 6BT, United Kingdom*

[3]*BENSC, Helmholtz Centre Berlin for Materials and Energy, D-14109 Berlin, Germany*

[4]*Laboratory for Quantum Magnetism, Ecole Polytechnique Fédérale de Lausanne, CH-1015 Lausanne, Switzerland*

[5]*Theoretische Physik, ETH–Hönggerberg, CH-8093 Zürich, Switzerland*

[6]*DPMC-MaNEP, University of Geneva, CH-1211 Geneva, Switzerland*

[7]*Centre de Physique Théorique, CNRS, Ecole Polytechnique, 91128 Palaiseau Cedex, France*

[8]*LPENSL, UMR 5672, CNRS, F-69364 Lyon Cedex 07, France*

[9]*Dipartimento di Fisica "E. R. Caianiello" and CNISM, Università di Salerno, I-84100 Salerno, Italy*

[10]*Institut Romand de Recherche Numérique en Physique des Matériaux (IRRMA), CH-1015 Lausanne, Switzerland*

[11]*Department of Chemistry and Biochemistry, University of Bern, CH-3000 Bern 9, Switzerland*

[12]*MPA-NHMFL, Los Alamos National Laboratory, Los Alamos, New Mexico 87545, USA*

[13]*Risø National Laboratory for Sustainable Energy, Technical University of Denmark, DK-4000 Roskilde, Denmark*

[14]*INAC/SPSMS/MDN, CEA–Grenoble and Université Joseph Fourier–Grenoble, F-38054 Grenoble, France*

(Received 2 September 2008; revised manuscript received 15 December 2008; published 30 January 2009)

Neutron diffraction is used to investigate the field-induced, antiferromagnetically ordered state in the two-leg spin-ladder material $(Hpip)_2CuBr_4$. This "classical" phase, a consequence of weak interladder coupling, is nevertheless highly unconventional: its properties are influenced strongly by the spin Luttinger-liquid state of the ladder subunits. We determine directly the order parameter (transverse magnetization), the ordering temperature, the spin structure, and the critical exponents around the transition. We introduce a minimal microscopic model for the interladder coupling and calculate the quantum fluctuation corrections to the mean-field interaction.

DOI: 10.1103/PhysRevB.79.020408 PACS number(s): 75.10.Jm, 75.25.+z, 75.30.Kz, 75.40.Mg

Low-dimensional magnets have been the subject of intense theoretical research for many decades. Of particular interest are the intriguing ground- and excited-state properties of one-dimensional (1D) systems such as chains and ladders.[1–7] In this context, residual interactions between the low-dimensional units, which are always present in real materials, may be viewed as a distraction from the intrinsic physics. However, such interactions open up fascinating new avenues of investigation concerning the crossover from one- to higher-dimensional behavior. In three dimensions (3D), antiferromagnetic (AF) magnons in a gapped quantum magnet undergo Bose-Einstein condensation (BEC) at a magnetic field B_c, where the gap is closed by the Zeeman effect.[8] At this quantum critical point, the spin components perpendicular to the magnetic field develop long-range order (3D-XY type). In contrast, in 1D any long-range order is destroyed by quantum phase fluctuations and a critical phase with algebraic spin correlations, a spin Luttinger liquid (LL), is predicted.[4,7] While the spin LL may be realized at finite temperatures in coupled $S=1/2$ chain systems such as $KCuF_3$,[9,10] a particularly rich phase diagram is expected for weakly coupled ladders: here the spin LL is induced from a gapped, quantum disordered (QD) phase by an applied magnetic field, and its LL parameters can be tuned directly by the field.[7]

Materials realizing quasi-1D spin-ladder geometries, and with critical fields B_c (QD to LL) and B_s (magnetic saturation) accessible in the laboratory, are rare.[3] While the latter difficulty is generally overcome in metal-organic compounds, these can still suffer from other complications, such as the additional terms found in the magnetic Hamiltonian of CuHpCl.[11] Thus the system $(C_5H_{12}N)_2CuBr_4$ $[(Hpip)_2CuBr_4]$ is unique in its class:[12,13] numerous thermodynamic measurements are in quantitative agreement with predictions for an ideal ladder,[14–16] and inelastic neutron scattering (INS) demonstrates a high degree of one dimensionality.[17] All of these techniques point to a minimal Heisenberg ladder Hamiltonian with respective rung and leg exchange constants $J_r=12.9(2)$ K and $J_l=3.3(3)$ K. Only nuclear magnetic resonance (NMR) measurements have to date been performed at temperatures low enough to access the energy scale of the interladder coupling: in Ref. 16, the transition to 3D order is found at and below 110 mK, and the phase boundary is interpreted in terms of a field-tuned spin LL regime between B_c and B_s.

Here we report the results of comprehensive neutron-diffraction studies, performed at dilution-refrigerator temperatures, of the 3D ordered phase in $(Hpip)_2CuBr_4$. We determine the spin structure and measure directly the transverse magnetic moment as a function of field and temperature. The vanishing of the order parameter, combined with the magnetocaloric effect (MCE), gives the LL crossover, the LL exponents close to the 3D regime, and independent measurements of the phase boundary. From the spin structure we deduce a microscopic model for the interladder coupling which allows a quantitative determination of the interaction between the

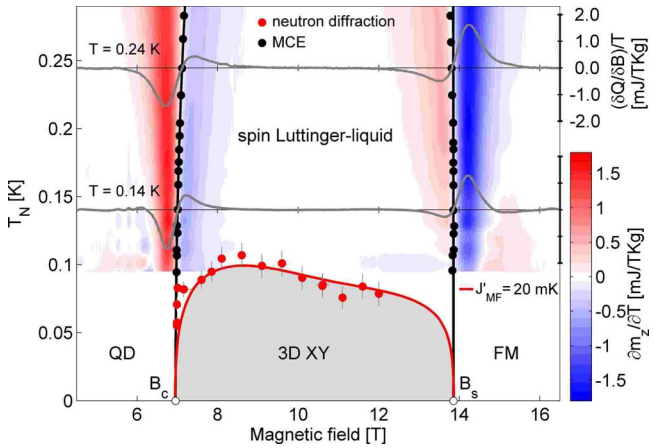

FIG. 1. (Color online) Low-T phase diagram of $(\mathrm{Hpip})_2\mathrm{CuBr}_4$. The crossover temperature to the spin-LL phase is derived from MCE measurements and the phase transition to the BEC (3D-XY magnetic order) from neutron diffraction. The contour plot is based on 18 individual field scans of the MCE (two shown as gray lines), using $(\delta Q/\delta B)/T=-(\partial m_z/\partial T)|_B$ (Ref. 15). The red line is based on a theoretical fit (see text).

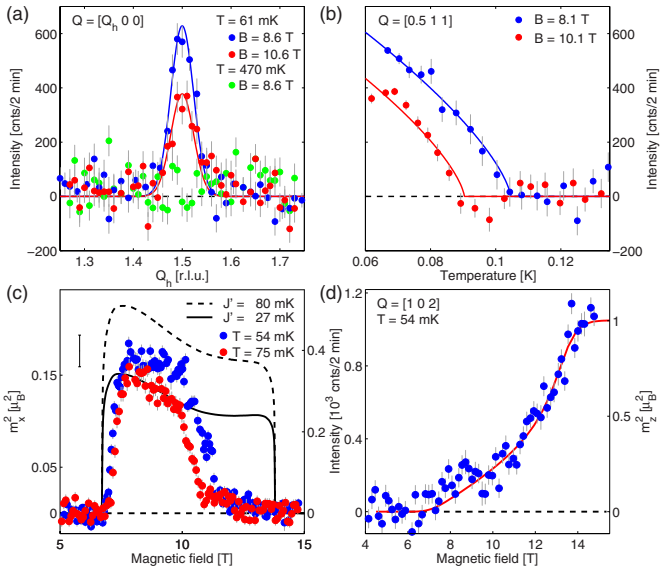

FIG. 2. (Color online) Summary of neutron-diffraction data. (a) Q-scans across an AF Bragg peak after subtraction of a flat background measured in the QD phase at $B=6$ T and $T=63$ mK. (b) T-dependence of the Bragg intensity, demonstrating the onset of 3D long-range order at $T_N(B)$; solid lines are fits using the 3D-XY exponent. (c) B-dependence of m_x^2 measured at $Q=(1.5\ 0\ 0)$ for $T=54$ mK (blue) and $T=75$ mK (red). Solid and dashed lines are from the DMRG MFA for the given interladder interaction J'. Error bars on data points are based on counting statistics, while the vertical black line indicates the systematic error of the calibration to absolute units. (d) Magnetic signal at $Q=(1\ 0\ 2)$, which is proportional to m_z^2: shown is the neutron intensity after subtraction of the nuclear contribution, which also corrects for magnetostriction effects. The red line is obtained from a QMC calculation.

1D subunits, using a combination of mean-field calculations[16] and quantum Monte Carlo (QMC) simulations of the full interacting-ladder model.

The MCE was measured on high-quality single-crystalline $(\mathrm{Hpip})_2\mathrm{CuBr}_4$ in a standard dilution refrigerator at the NHMFL in Los Alamos, with sweep rates between 0.025 and 0.075 T/min. Neutron-diffraction experiments were performed on deuterated $(\mathrm{Dpip})_2\mathrm{CuBr}_4$ single crystals with sample mass 200 mg on the instruments D23 at the ILL and RITA–2 at SINQ (PSI), using standard set-ups. For all measurements, a vertical magnetic field was applied along the crystallographic b axis, i.e., perpendicular to the ladders.

Before studying the 3D ordered phase, it is necessary to understand in full detail the disordered phase from which it emerges. The quasi-1D regime above the 3D phase boundary is investigated using the MCE, which maps the crossover from the QD state into the spin LL through local extrema in the temperature-dependence of the longitudinal magnetization m_z. Figure 1 shows $\partial m_z/\partial T$ (contour plot) and these extrema (black circles) for temperatures down to 100 mK, extending (from 300 mK) the results of our previous measurements[15] and providing a frame of reference for other reported results.[16] The LL crossover is analyzed by a sliding-window technique,[18] whose first step is the determination of the critical fields $B_c=6.96(2)$ T and $B_s=13.85(3)$ T. With these values fixed, the crossover temperature is fitted to $T_{\mathrm{LL}}\propto(B-B_c)^{1/\nu}$ (black lines), yielding an exponent $\nu=2.1(1)$ at B_c.[19] A ladder spin system in a field $B\approx B_c$ can be mapped to a free-fermion model (LL exponent $K=1$), and hence one expects $\nu=1$ (Ref. 5). However, a bosonization interpretation of density-matrix renormalization-group (DMRG) calculations for the ladder model[16] shows that $K(B)$ decreases rapidly below 1 as the field is moved away from B_c and B_s. Consequently, the true critical regime is very narrow, a result seen also in QMC calculations for the related Haldane spin chains.[20] Thus while our MCE measurements demonstrate spin LL behavior down to 100 mK, the universal exponents are not reached before the LL regime is cut off by 3D order. Close to the critical fields, our results indicate that the ladder system remains far from this universal regime even for $T/J_l\approx 0.03$.

Turning now to the ordered phase, Fig. 2 summarizes the results of our neutron-diffraction measurements, which were taken at temperatures down to 54 mK. Figure 2(a) shows Q-scans across the AF wave vector, $Q=(1.5\ 0\ 0)$, on cooling the sample from the spin-LL regime at $B_c<B<B_s$. Resolution-limited magnetic Bragg peaks are observed at base temperature, demonstrating long-range AF order. The magnetic Bragg peak remains at the same commensurate position, but its intensity decreases with increasing field, indicating a substantial field-dependence of the transverse ordered moment. The temperature-dependence of the Bragg intensity is presented in Fig. 2(b): the vanishing of the magnetic signal is used to determine the phase boundary shown as red circles in Fig. 1, and its thermal evolution is very well described by the critical exponent, $2\beta=0.70$, of the 3D-XY model[8] over the full range of data available (essentially $\frac{1}{2}T_N<T<T_N$).

Figure 2(c) shows field scans of the AF Bragg intensity at $Q=(1.5\ 0\ 0)$ for $T=54$ mK and $T=75$ mK. This is proportional to the square of the transverse magnetization, m_x^2, and was scaled to the ordered moment obtained at $B=8.6$ T from a complete refinement of the spin structure (below). In con-

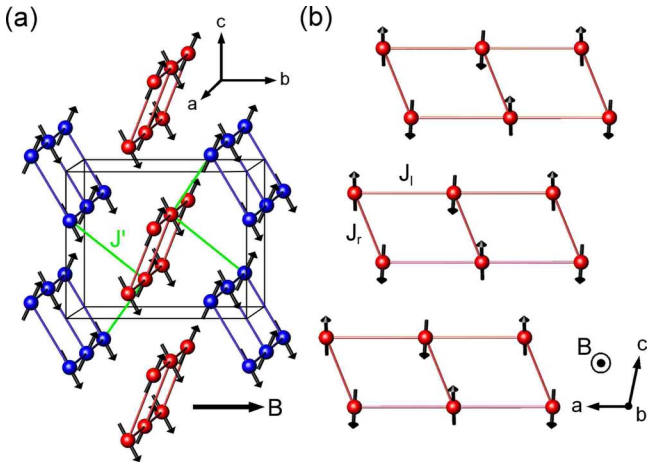

FIG. 3. (Color online) Magnetic structure (black arrows) in the 3D ordered phase of $(Dpip)_2CuBr_4$, determined by neutron diffraction at $B=8.6$ T and $T=63$ mK. Only Cu atoms forming the ladders are shown (red and blue). The spin component along the field ($B\|b$) is fixed by QMC calculations. Projections are shown (a) on the bc plane and (b) on the ac plane. Interladder bonds J' for one rung are shown in green.

trast to NMR, m_x^2 is determined directly by neutron scattering, allowing additional quantitative tests of theoretical predictions. From Fig. 2(b), the AF order parameter is not saturated at $T=54$ mK and no Bragg peak (or 3D transition) is observed for $B>12$ T. Above B_c, the uniform magnetization m_z increases monotonically, which generates a small, ferromagnetic (FM) signal on top of the nuclear Bragg peaks. Our characterization of all components of the magnetization is completed by field scans of this magnetic intensity, as shown in Fig. 2(d) for $\boldsymbol{Q}=(1\ 0\ 2)$. The red line is obtained from a QMC calculation of the ladder magnetization, m_z^2, using the exchange interactions cited above, and shows good overall agreement.

In addition to m_z and m_x, neutron diffraction also allows a quantitative determination of the magnetic structure. At base temperature and $B=8.6$ T (maximum $T_N\approx 110$ mK), the intensities of 26 AF Bragg peaks were recorded on D23. Among the four allowed magnetic structures, that shown in Fig. 3 provides the best fit ($\chi^2=5.54$): the spins are aligned perpendicular to the a axis and antiparallel within the ladder, but parallel on ladders of the same type [propagation vector $\boldsymbol{k}=(0.5\ 0\ 0)$]. The ordered moment is $0.41(2)\mu_B$ per copper ion. Its orientation is parallel to the maximum of the g factor in the ac plane.[12] We note that nearest-neighbor Cu atoms between adjacent ladders of opposite type (red and blue) have FM aligned spins [Fig. 3(a)].

A qualitative discussion of our results is aided by a specific model for the interladder coupling responsible for 3D order. Here we restrict our considerations to a minimal model with only one interladder interaction parameter, J', of magnitude $O(100$ mK). Inspection of the lattice structure of $(Hpip)_2CuBr_4$, which is similar to that of $TlCuCl_3$ (albeit with the dimer units rather less tilted relative to the ladder axis), motivates the choice of the bond J_3 in the notation of Ref. 21. This bond connects ladders of opposite orientations [red to blue in Fig. 3(a)] along directions $\pm(1\pm 0.5\ 0.5)$,

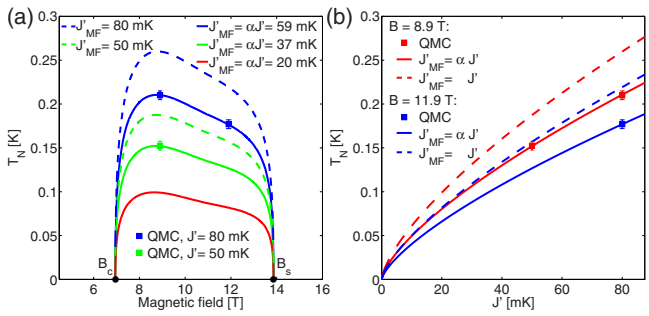

FIG. 4. (Color online) The 3D-XY phase boundary by DMRG MFA and QMC. (a) $T_N(B)$ for several values of J', as indicated, $\alpha=0.74(1)$. (b) T_N as a function of J'.

meaning that the Cu sites are displaced by one unit along the a axis. AF bonds $J'\equiv J_3$ then ensure the FM alignment mentioned above, and a completely unfrustrated spin structure. Any one ladder rung has four bonds of this type (coordination $z=4$). INS measurements of the very small triplet dispersions along the b and c axes tend to support this type of model; full details of the 3D spin dynamics and exchange paths will be presented elsewhere.[22]

The measured transition temperature $T_N(B)$ is shown in Fig. 1. The marked asymmetry about $B=(B_c+B_s)/2$ ($m_z=1/2$) arises from the changing influence of the upper two triplet branches as the field is increased, and is in strong contrast to spin systems in two and three dimensions, such as $BaCuSi_2O_6$ and $TlCuCl_3$.[8] This asymmetry is also apparent in QMC studies of coupled ladders.[23] The solid red line in Fig. 1 is fitted from the theory presented in Ref. 16: $T_N(B)$ depends on the LL parameters of the ladders, which are themselves functions of B and are obtained from a bosonization interpretation of DMRG calculations performed for a ladder with $J_r/J_l=3.6$. Interladder coupling is treated in a mean-field approximation (MFA), and the only free parameter in Fig. 1 is the magnitude of this exchange constant, J'_{MF}. The best fit to our experimental data yields $J'_{MF}=20(1)$ mK, providing valuable independent confirmation of the results in Ref. 16.

However, by its nature the MFA underestimates the effects of quantum fluctuations, and thus overestimates the value of T_N corresponding to a given J' [for coupled 1D chains by approximately 50% (Ref. 9)]. We have obtained the "bare" value of J' by performing QMC simulations[24,25] for the interladder exchange geometry of the minimal model, which is a very demanding computational task due to the strong spatial anisotropy of the exchange constants. It has been shown numerically[26] that quantitative agreement of mean-field and exact results can be recovered simply by introducing a renormalization factor α, which is a constant in the weak-coupling limit, and for the purposes of the current analysis can be viewed as a renormalization of the coupling $J'_{MF}=\alpha J'$. The 3D ordering temperature computed by QMC is shown in Fig. 4(a) at $B=8.9$ T for two chosen values of J' and $B=11.9$ T for one; the solid lines are obtained from the DMRG MFA. As shown in Fig. 4(b), a single value $\alpha=0.74(1)$ is indeed sufficient to ensure perfect agreement between the QMC simulations and the DMRG MFA. Hence the best fit to J'_{MF} corresponds to a bare (microscopic) coupling $J'=27(2)$ mK.

A further test of the coupling model and the DMRG MFA is provided by the transverse-moment measurements shown in Fig. 2(c). The qualitative shape of the zero-temperature, DMRG-based results is again asymmetric due to the changing influence of the high-lying triplet modes and to the field-dependence of the underlying LL parameters. While this appears to mirror the data, a quantitative comparison faces two complications: experimentally, the data is not in the low-temperature limit, and indeed falls unexpectedly above 10.5 T; theoretically, the calculated moment is rather insensitive to the value of J', while the quantum fluctuation suppression factor for m_x^2, which need not match that deduced from T_N, is unknown. Clearly even the unrenormalized value, $J'=27$ mK, somewhat underestimates the transverse moment, and significantly higher values, up to $J' \approx 80$ mK [Fig. 2(c)], appear to be required in this framework.[22] More detailed experiments and theoretical analysis will be necessary to resolve this discrepancy.

In summary, comprehensive neutron-diffraction data and measurements of the magnetocaloric effect are presented to investigate the 3D ordered phase realized in the prototypical spin-ladder material $(Hpip)_2CuBr_4$ at low temperatures and high magnetic fields. We determine the temperature of the transition which separates 1D from 3D physics in coupled spin Luttinger liquids, and characterize the critical behavior in the 1D regime. In the 3D phase, we measure both the transverse and longitudinal magnetizations, and establish the spin structure. The unconventional field-dependences of the Néel temperature and of the transverse magnetization agree well with a description based on a minimal coupling model and combining DMRG calculations with a mean-field treatment of the (renormalized) interladder interactions. We determine the renormalization factor for this coupled-ladder geometry by comparison with detailed QMC simulations.

We thank C. Berthier and M. Klanjsek for valuable discussions. This project was supported by the Swiss National Science Foundation through the NCCR MaNEP and Division II, by the Royal Society, the EPSRC, and the RTRA network "Triangle de la Physique." The NHMFL is supported by the NSF, the DOE, and the State of Florida. The work is based in part on experiments performed at the Swiss spallation neutron source, SINQ, at the Paul Scherrer Institute, Villigen, Switzerland.

[1] H. Bethe, Z. Phys. **71**, 205 (1931).
[2] F. D. M. Haldane, Phys. Lett. **93**, 464 (1983).
[3] E. Dagotto and T. M. Rice, Science **271**, 618 (1996).
[4] S. Sachdev, T. Senthil, and R. Shankar, Phys. Rev. B **50**, 258 (1994).
[5] R. Chitra and T. Giamarchi, Phys. Rev. B **55**, 5816 (1997).
[6] A. Furusaki and S.-C. Zhang, Phys. Rev. B **60**, 1175 (1999).
[7] T. Giamarchi and A. M. Tsvelik, Phys. Rev. B **59**, 11398 (1999).
[8] T. Giamarchi, Ch. Rüegg, and O. Tchernyshyov, Nat. Phys. **4**, 198 (2008), and references therein.
[9] H. J. Schulz, Phys. Rev. Lett. **77**, 2790 (1996).
[10] B. Lake, D. A. Tennant, C. D. Frost, and S. E. Nagler, Nature Mater. **4**, 329 (2005).
[11] M. Clémancey, H. Mayaffre, C. Berthier, M. Horvatic, J. B. Fouet, S. Miyahara, F. Mila, B. Chiari, and O. Piovesana, Phys. Rev. Lett. **97**, 167204 (2006).
[12] B. R. Patyal, B. L. Scott, and R. D. Willett, Phys. Rev. B **41**, 1657 (1990).
[13] B. C. Watson *et al.*, Phys. Rev. Lett. **86**, 5168 (2001).
[14] T. Lorenz, O. Heyer, M. Garst, F. Anfuso, A. Rosch, C. Rüegg, and K. Krämer, Phys. Rev. Lett. **100**, 067208 (2008).
[15] Ch. Rüegg *et al.*, Phys. Rev. Lett. **101**, 247202 (2008).
[16] M. Klanjšek *et al.*, Phys. Rev. Lett. **101**, 137207 (2008).
[17] B. Thielemann *et al.*, arXiv:0812.3880 (unpublished).
[18] O. Nohadani, S. Wessel, B. Normand, and S. Haas, Phys. Rev. B **69**, 220402(R) (2004).
[19] The exponent ν cannot be determined quantitatively at B_s because of strong contributions to the heat capacity from the Schottky anomaly of the nuclear spins (Ref. 15). The line in Fig. 1 is drawn with $\nu=2$.
[20] Y. Maeda, C. Hotta, and M. Oshikawa, Phys. Rev. Lett. **99**, 057205 (2007).
[21] M. Matsumoto, B. Normand, T. M. Rice, and M. Sigrist, Phys. Rev. B **69**, 054423 (2004).
[22] B. Thielemann *et al.* (unpublished).
[23] S. Wessel, M. Olshanii, and S. Haas, Phys. Rev. Lett. **87**, 206407 (2001).
[24] A. F. Albuquerque *et al.*, J. Magn. Magn. Mater. **310**, 1187 (2007).
[25] F. Alet, S. Wessel, and M. Troyer, Phys. Rev. E **71**, 036706 (2005).
[26] C. Yasuda, S. Todo, K. Hukushima, F. Alet, M. Keller, M. Troyer, and H. Takayama, Phys. Rev. Lett. **94**, 217201 (2005).